

Staging Blocked Evaluation over Structured Sparse Matrices

Pratyush Das
das160@purdue.edu
Purdue University
West Lafayette, Indiana, USA

Amirhossein Basareh
abasareh@purdue.edu
Purdue University
West Lafayette, Indiana, USA

Adhitha Dias
kadhitha@purdue.edu
Purdue University
West Lafayette, Indiana, USA

Artem Pelenitsyn
apelenit@purdue.edu
Purdue University
West Lafayette, Indiana, USA

Kirshanthan Sundararajah
kirshanthans@vt.edu
Virginia Tech
Blacksburg, Virginia, USA

Milind Kulkarni
milind@purdue.edu
Purdue University
West Lafayette, Indiana, USA

Ben Delaware
bendy@purdue.edu
Purdue University
West Lafayette, Indiana, USA

Abstract

The matrices used in many computational settings are naturally sparse, holding a small percentage of nonzero elements. Storing such matrices in specialized sparse formats enables algorithms that avoid wasting computation on zeros, significantly accelerating common matrix computations like sparse matrix-vector multiplication (SpMV) and sparse matrix-matrix multiplication (SpMM). In many real-world sparse matrices, however, nonzero elements are densely clustered in subregions of the matrix. For matrices that feature this sort of structured sparsity, hybrid formats can further improve performance by representing these subregions as dense blocks. Existing hybrid formats either fix the dimensions of dense blocks, padding irregular regions with zeros and wasting computation, or incur run-time overhead when iterating over variable-sized blocks.

This paper presents SABLE, a framework for accelerating structured sparse matrix computations by using staging to achieve the best of both of these approaches. Ahead of execution, SABLE inspects the matrix to identify variable-sized dense subregions, which it stores using a new hybrid format. It then eliminates the overhead typically associated with variable-sized blocks by using staging to generate specialized code that is amenable to vectorization. We evaluate SABLE on SpMV and SpMM kernels using matrices from the popular SuiteSparse data set. SABLE outperforms the best available SpMV baseline by $\sim 10\%$ on average, and SpMM baselines by $\sim 20\%$. When parallelized, SABLE achieves further speedups of up to $\sim 7\times$ on SpMV and SpMM over the best fully-sparse baseline when using 8 threads.

Keywords

Inspector-Executor, Code generation, Sparse Matrix-Vector multiplication, Sparse Matrix-Matrix multiplication

1 Introduction

Sparse matrices are ubiquitous in several computational domains, including machine learning, graph processing, and scientific computing [2, 5, 19, 41]. Since they have a large number of zero elements, using compressed storage formats to represent and compute over sparse matrices can lead to significant gains in memory usage and

computational performance. Common *sparse formats* like Compressed Sparse Row (CSR) [14] and Coordinate List (COO) [4] only store non-zero elements and use indirection arrays to implement matrix operations. However, these benefits come at a cost, as sparse kernels incur overhead when traversing the storage format's indirection arrays [49]. As a consequence, performance gains from sparse formats diminish as the ratio of zero to non-zero elements increases.

Real-world sparse matrices typically exhibit clusters of non-zero elements, resulting in variable sized dense regions that are distributed throughout the matrix (e.g., pruning neural networks [8]). These sorts of *structured sparse* matrices are better represented using storage formats that store only the dense blocks, e.g., Block Compressed Sparse Row (BCSR) [22]. These formats generalize the benefits of sparse formats to the block-level, so that common operations such as matrix multiplication [29] exhibit better memory access performance due to cache locality [56], thus improving upon formats that treat the whole matrix as sparse [7, 20]. BCSR, for example, stores entire blocks as dense, tolerating some zero elements within each block in exchange for regular memory access patterns. *Hybrid formats* take this further by enabling dense and sparse regions to be processed differently: dense regions are dispatched to a dense kernel while the remaining sparse regions are dispatched to a sparse kernel.

While existing approaches have demonstrated the effectiveness of this hybrid strategy, they have limitations that prevent them from fully exploiting the structured sparsity often found in real-world matrices. Chief among these is that most prior work assumed *fixed-size* blocks, whereas real-world matrices often feature dense regions of *varying sizes*: the matrix shown in Figure 1, for example, is best partitioned using a variable-sized grid, which more accurately captures its dense regions. Algorithms that operate over variable-sized blocks [39, 50] can better capture these regions, reducing the wasted computation over zero-padded elements that a fixed-size partitioning introduces. This flexibility comes at a cost, however, as iterating over variable-sized blocks is less efficient than for fixed-sized blocks, since the loop bounds are not known ahead of execution time [49].

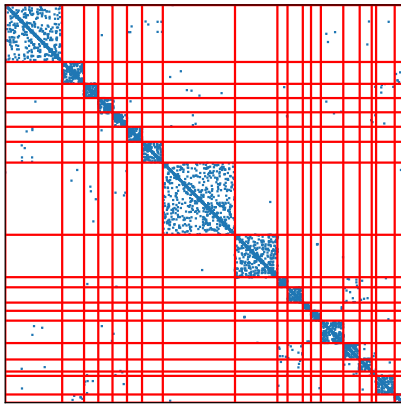


Figure 1: An example of a structured sparse matrix (*bcspr06*) found in the SuiteSparse benchmarks. Blue dots represent non-zero elements and the red lines capture the variable grid structure of the matrix.

One way to tackle this dilemma is to leverage the persistence of sparse matrix structure: while the non-zero values of a sparse matrix may change from invocation to invocation, in many scenarios—e.g., pruned neural networks—the structure of the sparse matrix stays fixed. As a result, code can be specially-generated based on the matrix structure; prior compilers [3, 9, 55] have used this approach to specialize generated code to the indices of individual non-zero elements. We observe that applying this same approach to the variable block size problem can yield highly efficient code: loop bounds and access patterns can be specialized per block, mitigating much of the overhead associated with variable-sized blocks. In particular, our approach allows entire dense regions to be dispatched to optimized kernels.

We implement this approach as a staging compiler, SABLE,¹ for structured sparse matrix computations. Our work combines two key techniques. First, we come up with a new hybrid storage format that allows variable-sized dense blocks to be stored separately from sparse regions, enabling efficient dispatch. Second, we use a staging approach that generates and compiles code specialized to the structure of the matrix, eliminating abstraction overheads. SABLE analyzes the structure of a sparse matrix and generates specialized code based on the structure of that matrix, enabling different regions of the matrix to be handled using different execution strategies. On the SuiteSparse benchmark suite, this approach outperforms the best fully-sparse baseline by ~10% on average for SpMV and ~20% for SpMM, with gains on some benchmarks of up to 2× and 2.6×, respectively.

A crucial step in this pipeline is identifying matrix subregions that contain a high ratio of number of non-zero to number of zero elements ahead of time, so that SABLE can generate code specialized to these blocks using staging [47]. We call such blocks δ -dense, where at least $\delta\%$ of the elements are non-zero. In addition, determining whether a δ -dense block would benefit from being processed by a dense kernel depends on several factors, including their size and shape, making this an expensive operation to perform

online. To address this challenge, we propose a novel partitioning algorithm that first inspects a matrix to determine whether it is likely to benefit from our approach and, if so, partitions it into a set of variable-sized δ -dense blocks using a variable-sized grid that more effectively captures blocks that can be processed by a dense kernel.

To represent the result of this partitioning, SABLE introduces a new storage format called VBR-C (Variable Block Row Compressed). VBR-C is a hybrid format that stores δ -dense regions of the matrix using a Variable Block Row (VBR) representation [39], while storing the remaining sparse regions in a sparse format chosen by the user. This representation allows SABLE to efficiently specialize code for δ -dense blocks while delegating sparse blocks to an existing sparse kernel. Operating over VBR-C further enables the compiler to generate vectorized kernels for δ -dense blocks, as their elements are stored in contiguous memory. An additional benefit of our design is that sparse regions can be dispatched to an existing sparse library appropriate for that workload, including any state-of-the-art library that may emerge in the future, while still gaining the benefits of treating part of the matrix as dense.

In summary, this paper presents the following contributions:

- An automatic partitioning algorithm that identifies whether a structured sparse matrix computation would benefit from SABLE, and if so, decomposes the matrix into variable-sized δ -dense blocks. (Section 3)
- A new hybrid storage format, VBR-C, that stores δ -dense subregions of the matrix as variable sized blocks (VBR), and the remainder in a sparse format chosen by the user. (Section 4)
- SABLE: A staging compiler that generates code specialized to the features of the δ -dense blocks of a matrix (Section 5).
- Evaluation of SpMV and SpMM over real world sparse matrices that shows speedups over state-of-the-art systems. (Section 6)

2 Overview

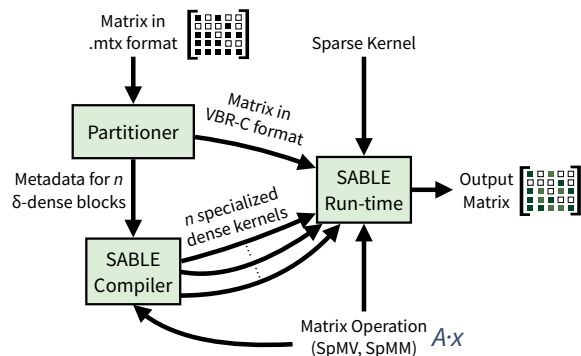


Figure 2: Overview of SABLE

Figure 2 provides a high-level overview of our pipeline. The system takes a sparse matrix in the Matrix Market (.mtx) format as input, which SABLE then partitions into variable-sized blocks, which are then stored in the Variable Block Row-Compressed (VBR-C) storage format.

¹SABLE – StAging BLocked Evaluation over Structured Sparse Matrices

The VBR-C metadata for the δ -dense blocks is then passed to SABLE’s compiler, which analyzes the shapes of the blocks and generates specialized dispatch code for the given operation. Depending on the block dimensions, the dense blocks are dispatched to optimized BLAS routines (e.g., `cb1as_dgemv` for SpMV or `cb1as_dgemm` for SpMM) or to a custom library of shape-specialized handwritten kernels (Section 5). At a high level, SABLE specializes the code operating over a δ -dense block based on a set of its features (rows, columns, and δ). If the block has a high δ (i.e. it is mostly dense), it is able to generate the most performant kernel dispatch for that block. Note that when $\delta < 1$, dispatching a δ -dense block to a dense kernel necessarily involves computing over some zeroes. Nevertheless, the efficiency advantage of dense computation means that for a wide range of δ (empirically observed as $\delta > .5$), the “wasted” work is outweighed by the efficiency gain. When a block has low δ (i.e. it is mostly sparse), SABLE generates code that dispatches those blocks to a sparse kernel of the user’s choosing. SABLE does not generate any code for blocks that are empty, skipping the computation over those blocks entirely. This allows SABLE to generate efficient code even if the sparse matrix is not perfectly partitioned into a set of δ -dense blocks: as Figure 1 shows, real-world matrices have all three types of blocks.

SABLE follows the inspector-executor paradigm [35]: the partitioner and staging compiler form the inspector, which analyzes the matrix structure and generates specialized code, while the runtime serves as the executor, dispatching each block to the appropriate kernel. We discuss the inspector-executor model and related approaches in Section 7. The SABLE runtime receives the specialized block kernels, the full VBR-C representation (both the indirection arrays and the dense block values), the remaining sparse region stored in a standard sparse format (e.g., CSR), a user-specified sparse kernel for that format, and the operation to perform (currently SABLE supports SpMV and SpMM). The sparse kernel is a parameter of the system, allowing users to leverage any current or future state-of-the-art sparse library. The runtime executes the specialized kernels over the dense blocks and the user-supplied sparse kernel over the sparse region, producing the output tensor (a vector for SpMV or a matrix for SpMM).

3 Partitioner

This section describes the heuristic partitioner we use to convert a sparse matrix into the VBR-C layout (Section 4). The main goal of the partitioner is to find non-overlapping high-density δ -dense blocks.

Partitioning a sparse matrix into the optimal number of high δ -dense regions is an NP-hard problem [34]. However, we use some heuristics to find a good approximation of the optimal partitioning and maximize the number of dense blocks. In particular, our partitioner applies a fixed similarity threshold—serving as an approximation for the lower bound on block density—to identify large contiguous blocks. Although the threshold is chosen statically irrespective of the input matrix, the approach reliably works across diverse datasets without requiring case-specific tuning, resulting in a robust and interpretable framework. The key design elements are:

- A minimum density threshold of 50%: this reflects the empirically observed break-even point where the cost of computing over padded zeros is offset by the performance of dense kernels.
- A minimum area threshold A_{\min} : this ensures blocks are large enough to amortize the overhead of switching between dense and sparse code paths. As a performance tweak, the block search (Algorithm 2) requires the outer dimension—rows for CSR, columns for CSC—to be at least $\lceil \sqrt{A_{\min}} \rceil$; any span shorter than this cannot reach the area threshold, so it is skipped. Because this constraint is applied only to the outer dimension of each representation, blocks whose inner dimension is smaller than $\lceil \sqrt{A_{\min}} \rceil$ are still possible. In our implementation, $A_{\min} = 2500$, giving a minimum outer span of 50.
- A scoring function, $\text{score}(B) = \text{area}(B) \cdot (\text{density}(B) - 0.5)^{1.5}$ where $\text{density} > 0.5$, that prefers denser blocks while still accounting for size; the super-linear exponent favors blocks with substantially higher density over larger but marginally dense blocks.

Algorithm 1 shows the overall partitioning procedure. The algorithm takes the matrix in both CSR and CSC representations and recursively decomposes it into δ -dense blocks. For each rectangular region, the block search subroutine (Algorithm 2) is invoked on both the CSR and CSC representations—some blocks are discovered more naturally by iterating along rows than columns—and the higher-scoring result is kept. Once a valid block is found, its rows and columns are marked as *used* and the algorithm recurses on the four surrounding sub-regions: above, below, left, and right of the accepted block. A strong exclusion invariant ensures that no two accepted blocks share any row or column, guaranteeing a non-overlapping partition compatible with the VBR-C format (Section 4). Before acceptance, a trimming step iteratively removes boundary rows or columns whose deletion improves the block’s overall density, evaluating all four edges until no single-edge removal helps. After the recursive decomposition completes, blocks with a single column ($N \times 1$) are discarded, as they cannot benefit from dense execution because in SABLE’s current implementation, δ -dense blocks are dispatched to kernels that iterate over rows. Finally, the matrix is deemed suitable for SABLE’s code generation only if at least 10% of its nonzeros are covered by accepted blocks; matrices below this threshold lack sufficient dense structure to justify VBR-C conversion.

The core subroutine is the dense block search shown in Algorithm 2. For a given region and compressed matrix representation (CSR or CSC), the algorithm sweeps over all starting positions along the *outer* dimension—rows for CSR, columns for CSC. For each starting position o_0 , it incrementally extends the outer span by advancing o_1 , accumulating a histogram H that records, for each inner-dimension index, the count of nonzeros across the current span $[o_0, o_1]$. A two-pointer sliding window over H then identifies the inner-dimension range that maximizes the block score: when the window’s density falls below 0.5, the left pointer advances to shrink the window; when the area constraint is not yet met, the right pointer advances to expand it. The two-pointer scan is amortized linear in the inner dimension, so the total work per starting position is dominated by the cost of histogram construction.

Algorithm 1 Partitioner**Require:** CSR and CSC representations of matrix A

```

1: function PARTITION( $A$ )
2:   DECOMPOSE( $[0, \text{nrows}] \times [0, \text{ncols}]$ )
3:   Discard all blocks  $B$  with  $\text{width}(B) = 1$ 
4:   if  $\sum_B \text{nnz}(B) < 0.1 \times \text{nnz}(A)$  then reject  $A$ 
5:   return accepted blocks

6: function DECOMPOSE( $R = [r_0, r_1] \times [c_0, c_1]$ )
7:   if  $\text{area}(R) < A_{\min}$  then return
8:    $B \leftarrow \text{FINDBLOCK}(A_{\text{CSR}}, R)$ 
9:    $B' \leftarrow \text{FINDBLOCK}(A_{\text{CSC}}, R)$ 
10:  if  $\text{score}(B') > \text{score}(B)$  then  $B \leftarrow B'$ 
11:  if  $\text{area}(B) < A_{\min}$  then return
12:  if any row or column of  $B$  is already used then return
13:  TRIM( $B$ ) ▷ Remove low-density edges
14:  if  $\text{density}(B) < 0.5$  or  $\text{area}(B) < A_{\min}$  then return
15:  Accept  $B$ ; mark its rows and columns as used
16:  DECOMPOSE( $[r_0, B.r_0] \times [c_0, c_1]$ ) ▷ Above
17:  DECOMPOSE( $[B.r_1, r_1] \times [c_0, c_1]$ ) ▷ Below
18:  DECOMPOSE( $[B.r_0, B.r_1] \times [c_0, B.c_0]$ ) ▷ Left
19:  DECOMPOSE( $[B.r_0, B.r_1] \times [B.c_1, c_1]$ ) ▷ Right

```

Parallelization. The outer loop of Algorithm 2 is parallelized with OpenMP using dynamic scheduling. Each thread maintains a private histogram and thread-local best candidate; after all iterations complete, thread-local results are merged via a critical section to determine the global best.

Practical considerations. For exceptionally large or irregular matrices, the partitioner enforces a timeout (4 hours in our experiments), after which it terminates and returns the blocks found so far. All but 1 matrix in our benchmark suite complete within this budget.

4 Variable Block Row Compressed

The Variable Block Row (VBR) format [28, 39] organizes a sparse matrix by grouping its rows and columns into blocks of varying sizes, allowing regions of dense data to be stored and processed more efficiently. The benefit of VBR is that it can create non-uniformly sized blocks around dense regions to better capture the structure of the matrix. An important property of the VBR format is that the row and column splits span the entire matrix—parts of the matrix cannot be split differently. VBR uses indirection arrays to record the block row and column boundaries, the starting index of each block in a contiguous value array, and which blocks appear in each block row. Every block—regardless of its density—is stored as a dense sub-matrix in the value array, with all zeros within blocks explicitly represented.

However, VBR is not a perfect fit for SABLE’s premise of storing and operating over high δ -dense and low δ -dense blocks separately. If a block contains even a single non-zero value, VBR stores the entire block as dense, including all zero values. This can lead to a significant increase in memory usage, especially for matrices with

Algorithm 2 Dense Block Search**Require:** Compressed matrix M (CSR or CSC); region R

```

1: function FINDBLOCK( $M, R$ )
2:    $B.\text{score} \leftarrow -1$ ;  $s_{\min} \leftarrow \lceil \sqrt{A_{\min}} \rceil$  ▷ Prune: outer span below
   this cannot reach minimum area
3:   parallel for each outer start  $o_0$  in  $R$  do
4:      $H[0 \dots L_{\text{in}}-1] \leftarrow 0$  ▷ Thread-local histogram
5:     for  $o_1 \leftarrow o_0$  to outer end of  $R - 1$  do
6:       for each  $\text{nnz}$  at inner index  $j$  in slice  $o_1 \cap R$  do
7:          $H[j] \leftarrow H[j] + 1$ 
8:          $s \leftarrow o_1 - o_0 + 1$ 
9:         if  $s < s_{\min}$  then continue
10:         $\text{nnz} \leftarrow 0$ ;  $i_0 \leftarrow 0$ 
11:        for  $i_1 \leftarrow 0$  to  $L_{\text{in}} - 1$  do
12:           $\text{nnz} \leftarrow \text{nnz} + H[i_1]$ 
13:          while  $i_0 \leq i_1$  do
14:             $a \leftarrow s \times (i_1 - i_0 + 1)$  ▷ Block area
15:            if  $a < A_{\min}$  then break
16:             $d \leftarrow \text{nnz} / a$  ▷ Block density
17:            if  $d \geq 0.5$  then
18:               $sc \leftarrow a \cdot (d - 0.5)^{1.5}$ 
19:              if  $sc > B.\text{score}$  then update  $B$ 
20:              break
21:             $\text{nnz} \leftarrow \text{nnz} - H[i_0]$ ;  $i_0 \leftarrow i_0 + 1$ 
22:          end parallel for ▷ Merge thread-local results
23:   return  $B$ 

```

large blocks. If a compiler were to index into only the non-zero values of the block, the non-contiguous access pattern would cause many cache misses, leading to poor performance.

To solve these problems, we introduce the Variable Block Row Compressed (VBR-C) format. Our VBR-C representation employs a hybrid strategy that combines the strengths of VBR and a sparse format of the user’s choice. Unlike BCSR (which uses fixed blocks) and UBCSR (which uses unaligned blocks that may incur fill-in), as well as the reduced CSR method by Shantharam et al. [42], VBR-C differentiates dense substructures from sparse regions by applying a VBR-like scheme to dense areas and storing the sparse remainder in any standard sparse format. In our evaluation we use CSR for the sparse regions, but the format is agnostic to this choice; any sparse representation (e.g., COO, CSC, or ELL) can be substituted.

Figure 3 shows an example of a matrix stored in the VBR-C format. VBR-C retains the same structural indirection arrays as VBR— Rpnr , Cpnr , Bpnr , Bpntrb , Bpntrc , Bindx , and Indx —so that the block row and column boundaries, the number of blocks per block row, and the block column indices are represented identically. The key difference lies in how each block’s values are stored. In VBR, every block is stored densely in the Val array, including blocks that are mostly zeros. In VBR-C, only blocks that meet the density threshold are stored as dense sub-matrices in the Val array; their values are omitted for blocks below the threshold. Instead, the non-zero values of sparse blocks are stored collectively in a separate set of CSR arrays: indptr (the row pointer array), indices (the column

| | | | | | | | | | | |
|----|---|----|---|---|----|----|----|---|----|----|
| 4 | 2 | 0 | 0 | 0 | 1 | 0 | 0 | 0 | 0 | 1 |
| 1 | 5 | 0 | 0 | 0 | 2 | 0 | 0 | 0 | 0 | -1 |
| 0 | 0 | 6 | 1 | 2 | 2 | 0 | 0 | 0 | 0 | 0 |
| 0 | 0 | 2 | 7 | 1 | 0 | 0 | 0 | 0 | 0 | 0 |
| 0 | 0 | -1 | 2 | 9 | 3 | 0 | 0 | 0 | 0 | 0 |
| 2 | 1 | 3 | 4 | 5 | 10 | 4 | 3 | 2 | 0 | 0 |
| 0 | 0 | 0 | 0 | 0 | 4 | 13 | 4 | 2 | 0 | 0 |
| 0 | 0 | 0 | 0 | 0 | 3 | 3 | 11 | 3 | 0 | 0 |
| 0 | 0 | 0 | 0 | 0 | 0 | 2 | 0 | 7 | 0 | 0 |
| 8 | 4 | 0 | 0 | 0 | 0 | 0 | 0 | 0 | 25 | 0 |
| -2 | 3 | 0 | 0 | 0 | 0 | 0 | 0 | 0 | 8 | 0 |

(a) Matrix partitioned into Variable Block Rows.

- Val: [4, 1, 2, 5, 1, 2, 6, 2, -1, 1, 7, 2, 2, 1, 9, 2, 1, 3, 4, 5, 10, 4, 3, 2, 13, 3, 2, 4, 11, 0, 2, 3, 7, 8, -2, 4, 3]. Contains the values of the dense blocks in column-major order.
- Indx: [0, 4, 6, 10, 19, 22, 24, 27, 28, 31, 34, 43, 47, 51]. Contains the starting index of each dense block in the Val array. The array is inclusive of the length of the Val array.
- Bindx: [0, 2, 4, 1, 2, 0, 1, 2, 3, 2, 3, 0, 4]. Contains the indices of the blocks in each block row.
- Rpntr: [0, 2, 5, 6, 9, 11]. Contains the starting index of each block row.
- Cpntr: [0, 2, 5, 6, 9, 11]. Contains the starting index of each block column.
- Bpntrb: [0, 3, 5, 9, 11]. Contains the number of nnz blocks till the start of this block row.
- Bpntr: [3, 5, 9, 11, 13]. The difference between each value in Bpntrb and Bpntr gives us the number of dense blocks in each block row.
- ublocks: [2, 4, 9, 12]. Index of blocks that are stored as CSR.
- indptr: [0, 1, 2, 3, 3, 4, 4, 5, 6, 6, 7, 8]. CSR index pointer array.
- indices: [10, 10, 5, 5, 5, 5, 9, 9]. CSR column index array.
- csr_val: [1, -1, 2, 3, 4, 3, 25, 8]. CSR values array.

(b) Indirection arrays for the VBR matrix.

Figure 3: Matrix represented in the Variable Block Row Compressed format.

index array), and *csr_val* (the values in row-major order). An additional *ublocks* array records which blocks are stored in this sparse representation. This hybrid approach reduces memory usage by avoiding the explicit storage of zeros in sparse blocks, and enables SABLE to dispatch each block type to the appropriate kernel.

5 Staging compiler

SABLE adopts a multi-stage compilation process that uses the sparse structure of the matrix to generate a specialized intermediate program, that is then compiled further. Note that this process is independent of the particular values of the non-zero elements of a matrix. As a consequence, SABLE generates programs that can operate over different matrices that have the same sparsity structure.

Staging [47] compilers generate specialized code based on information available at compile time. The simplest form of staging is partially evaluating a function when a subset of its arguments are known at compile time, resulting in a new function optimized for the arguments provided at runtime. Consider the following loops that perform SpMV over a sparse matrix stored in CSR format:

```

1 for i in range(num_rows):
2     for j in range(row_ptr[i], row_ptr[i+1]):
3         y[i] += val[j] * x[col_idx[j]]

```

If *row_ptr* and *col_idx* are known at compile time (as they are for a given sparse matrix) and the column indices within a block are contiguous, a staging compiler can partially evaluate the loops to eliminate the indirection arrays and produce code with fixed bounds. For example, specializing for a row where *row_ptr[i]* is 7, *row_ptr[i+1]* is 10, and the column indices are contiguous starting at 5 yields:

```

1 for j in range(5, 8):
2     y[3] += val[7 + j - 5] * x[j]

```

The resulting loop accesses contiguous memory and is directly vectorizable by standard compilers, unlike the original indirection-based loop. SABLE applies this principle at the block level: since the

```

1 y=[0]*len(x)
2 count=0
3 for a in range(len(rpnter)-1):
4     if bpnter[a]==-1:
5         continue
6     valid_cols=bindx[bpnter[a]:bpnter[a+1]]
7     for b in range(len(cpnter)-1):
8         if b in valid_cols:
9             start_val=val[indx[count]]
10            r1=range(rpnter[a], rpnter[a+1])
11            r2=range(cpnter[b], cpnter[b+1])
12            spmv(start_val, r1, r2, x, y)
13            count+=1
14
15 def spmv(val, row_range, col_range, x, y):
16     for i in row_range:
17         for j in col_range:
18             col=j-col_range.start
19             row=i-row_range.start
20             y[i]+=val[col*len(row_range)+row]*x[j]
21     return y

```

Figure 4: SpMV over non-empty blocks (Stage 0)

VBR indirection arrays are known at staging time, SABLE partially evaluates the block traversal code to produce specialized dispatch calls with fully determined coordinates and offsets.

SABLE receives the VBR-C indirection arrays (e.g., *rpnter*, *cpnter*, *bpnter*, *bpnter*, *bindx*, *indx*) from the partitioner as metadata describing the δ -dense block structure. These indirection arrays are derived from the dense block coordinates identified by the partitioner. At staging time, SABLE analyses these indirection arrays to extract dense subregions in the given sparse matrix. SABLE then generates C code that dispatches each dense block to an appropriate kernel for the given operation. We discuss below how SABLE integrates these in various stages with its code generator to produce efficient code.

Stage 0 (Python DSL). SABLE is provided with the storage format indirection arrays. SABLE, in conjunction with its block iteration algorithm, traverses the indirection arrays and determines a dispatch strategy for each δ -dense block. Since the block dimensions are derivable from the indirection arrays at this stage, large blocks with favorable aspect ratios are dispatched to optimized BLAS routines, while smaller or irregularly shaped blocks are dispatched to shape-specialized handwritten kernels. The block iterator cannot directly apply the user-provided function to each block because complete information about the block, e.g., block coordinates and the index into the value array, is not available at Stage 0. The block iterator is responsible for traversing the storage format indirection arrays and extracting the dense subregions of the matrix. For example, Figure 4 shows an SpMV snippet that the user would write over a sparse matrix stored in the VBR format without SABLE. The VBR parameters (`valid_cols`, `cpntr`, `rpntr`, `indx`, and `count`) are either known or calculable at Stage 0. Hence, we can partially evaluate these values and generate specialized code at Stage 1.

Stage 1 (C). At Stage 1, the coordinates of each dense subregion and the offsets into the value array have been fully resolved, allowing SABLE to emit the appropriate dispatch calls. For SpMV, large dense blocks are dispatched to `cblas_dgemv`, while smaller blocks are dispatched to handwritten kernels that exploit the specific block shape (e.g., single-row or single-column optimizations). For SpMM, the corresponding dispatch targets are `cblas_dgemm` for large blocks and shape-specialized handwritten kernels for smaller blocks. Figure 5 below shows an example handwritten SpMV kernel that SABLE dispatches to, with the block coordinates (`i = 640 : 690`; `j = 4175 : 4235`) and value array offset (`val[69722+ ...]`) fully resolved. Figure 6c illustrates this hybrid dispatch for an example SpMV operation.

```

1 ....
2 for (int i=640; i<690; i++)
3   for (int j=4175; j<4235; j++)
4     y[i]+=val[69722+(j-4175)*50+i-640]*x[j];
5 ....
    
```

Figure 5: Handwritten SpMV kernel dispatched to by SABLE (Stage 1)

Figure 6 shows a sparse matrix and two ways of performing SpMV over it. The matrix (Figure 6a) has non-zero elements that can be grouped into blocks of varying density. The code generated (Figure 6b) for an SpMV operation over the matrix if it was stored in the CSR format operates only over non-zeros and is not vectorizable by a standard compiler due to the indirect accesses to the `A_val` array. It also does not take advantage of the structure of grouped non-zero elements of the matrix. Instead, SABLE takes advantage of the block structure and dispatches each δ -dense block to an appropriate kernel based on its dimensions (Figure 6c). Dense blocks with favorable dimensions are dispatched to `cblas_dgemv`, while smaller dense blocks are dispatched to shape-specialized handwritten kernels. The remaining sparse blocks are merged into a single CSR region and dispatched to a user-supplied sparse kernel. Each dispatch in Figure 6c is highlighted in the same color as its corresponding block(s) in the matrix.

| | | | | | | | | |
|---|---|---|---|---|---|---|---|---|
| x | x | x | x | 0 | 0 | 0 | x | 0 |
| x | x | x | x | 0 | 0 | x | 0 | 0 |
| 0 | 0 | 0 | 0 | 0 | 0 | 0 | 0 | 0 |
| x | x | x | x | 0 | 0 | x | 0 | 0 |

(a) Sparse Matrix A

```

1 for (int i=0; i<rows; i++)
2   for (int j=A_rp[i]; j<A_rp[i+1]; j++)
3     y[i]+=A_val[j]*x[A_cols[j]];
    
```

(b) SpMV over A stored in CSR format

```

1 cblas_dgemv(CblasColMajor, CblasNoTrans,
2            2, 4, 1.0, &A_val[0], 2,
3            &x[0], 1, 1.0, &y[0], 1);
4 for (int j=0; j<4; j++) y[3] += A_val[8+j]*x[j];
5 sparse_spmv(A_csr, x, y);
    
```

(c) SABLE dispatch for SpMV over A

Figure 6: Different ways to perform an SpMV operation over a sparse matrix.

6 Evaluation

Our evaluation of this approach considers 3 key questions:

- **RQ1** How do the performance improvements of SABLE compare to that of prior approaches?
- **RQ2** Does our technique scale well with multiple threads?
- **RQ3** How much does each of the components of our partitioner contribute to its ability to identify regions that can be accelerated by dense kernels?

Experimental setup. All experiments were conducted on a single-socket Intel(R) Xeon(R) w7-3445 system with 20 physical cores (20 hardware threads), each running at up to 4.8 GHz. The system has 52.5 MiB of shared L3 cache, 40 MiB of total L2 cache (2 MiB per core), and 48 KB of L1 data cache per core. Each program was compiled using GCC v11.4.0 with the `-O3 -march=native -funroll-all-loops -mavx -mprefer-vector-width=512` optimization flags. For SpMV, each generated benchmark binary performs 30 timed iterations internally and is invoked 30 times, yielding 900 samples per configuration; this higher sample count is necessary because SpMV’s shorter runtimes make it more susceptible to system noise. We remove outliers using decile filtering and report the mean of the remaining samples. For SpMM, the binary performs 10 internal iterations and is invoked 10 times (100 samples per configuration), as the longer per-invocation runtimes produce more stable measurements.

Benchmark construction. We evaluate SABLE using SuiteSparse [12], a publicly available set of sparse matrices drawn from real-world applications. To identify structured sparse matrices in this set, we applied our partitioner to 1,578 SuiteSparse matrices containing between 15,000 and 5,000,000 non-zero elements. Our partitioner identified δ -dense blocks in 128 of these matrices; we randomly selected 70 of these to use in our evaluation. These matrices range from 18,552 to 2.3 million non-zeros, with dimensions varying from small ($1,176 \times 1,176$) to large ($27,607 \times 27,607$) square matrices, as well as highly rectangular ones (up to $4,350 \times 104,374$). The number of δ -dense blocks identified ranges from 1 to 34, with average block

Table 1: Comparison of SABLE against other approaches for sparse matrix computation on 30 SuiteSparse matrices identified by our partitioner as potentially benefiting from our approach. The first group of columns gives the salient features of each benchmark: rows, columns, non-zeros, number of δ -dense blocks (*BL*), average block density (*Avg. dens.*), and non-zeros in blocks (*Bl. Nnz*, % *Nnz*). The next two groups of columns reports the performance improvement of SABLE over each baseline on SpMV and SpMM computations, respectively (time in μ s and speedup). The highest speedup for each benchmark is given in bold; the lowest time is underlined.

| Matrix | Matrix Features | | | | | | SABLE speedup over individual baselines | | | | | | |
|--------------------|-----------------|---------|-----------|----|-------|-------------------|---|--------------------|----------------------|------------------------|-------------------------|---------------------------------|---------------------------------|
| | | | | | | | SpMV | | | | SpMM | | |
| | | | | | | | SpV8 | MKL | Naive | UZP | SpReg | Naive | MKL |
| eris1176 | 1,176 | 1,176 | 18,552 | 3 | 67.7 | 10,428 (56.2%) | <u>6</u> (1.04×) | 7 (1.09×) | 6 (1.17×) | 11 (1.47 ×) | 2,691 (1.00×) | 849 (1.59×) | <u>822</u> (1.62 ×) |
| c-30 | 5,321 | 5,321 | 65,693 | 2 | 94.6 | 27,532 (41.9%) | <u>18</u> (1.15×) | 24 (1.09×) | 24 (1.10×) | 42 (1.44 ×) | 25,903 (1.05×) | <u>5,058</u> (1.39×) | 5,486 (2.02 ×) |
| lowThrust_3 | 7,064 | 7,064 | 80,645 | 2 | 100.0 | 10,976 (13.6%) | <u>26</u> (1.05×) | 32 (0.99×) | 29 (1.12×) | 49 (1.19 ×) | 39,524 (1.02×) | <u>10,512</u> (0.95×) | 8,708 (1.07 ×) |
| jendrec1 | 2,109 | 4,228 | 89,608 | 1 | 55.9 | 78,935 (88.1%) | <u>23</u> (1.64×) | 27 (0.96×) | 24 (1.14×) | 27 (1.79 ×) | 14,105 (0.91×) | <u>3,065</u> (2.14 ×) | 2,926 (2.09×) |
| orani678 | 2,529 | 2,529 | 90,158 | 1 | 86.1 | 39,081 (43.3%) | <u>24</u> (1.21×) | 26 (1.12×) | 26 (1.09×) | 41 (1.31 ×) | 10,436 (1.02×) | <u>4,951</u> (1.41 ×) | 6,604 (1.32×) |
| vsp_c-30_data_data | 11,023 | 11,023 | 124,368 | 2 | 94.6 | 27,532 (22.1%) | <u>46</u> (1.13×) | 49 (1.02×) | 61 (1.05×) | 94 (1.21 ×) | 141,436 (1.02×) | <u>12,722</u> (1.13×) | <u>10,363</u> (1.47 ×) |
| lp_osa_07 | 1,118 | 25,067 | 144,812 | 1 | 73.5 | 17,609 (12.2%) | <u>62</u> (1.01 ×) | 49 (1.01×) | <u>46</u> (1.01×) | 213 (0.96×) | 52,359 (0.92×) | <u>37,442</u> (0.99×) | 88,500 (1.12 ×) |
| lowThrust_4 | 13,562 | 13,562 | 160,947 | 2 | 100.0 | 21,084 (13.1%) | 65 (1.04×) | <u>63</u> (1.06×) | 66 (1.01×) | 97 (1.21 ×) | 33,796 (0.97×) | <u>24,537</u> (0.95×) | <u>19,960</u> (1.05 ×) |
| c-45 | 13,206 | 13,206 | 174,452 | 5 | 87.7 | 45,009 (25.8%) | <u>65</u> (1.11×) | 69 (1.02×) | 65 (1.02×) | 120 (1.28 ×) | 206,740 (1.00×) | <u>19,763</u> (1.13×) | 23,155 (1.36 ×) |
| brainpc2 | 27,607 | 27,607 | 179,395 | 2 | 100.0 | 55,192 (30.8%) | <u>77</u> (1.11×) | 97 (0.94×) | <u>76</u> (1.06×) | 118 (1.60 ×) | 823,455 (1.01×) | <u>36,090</u> (1.02×) | 37,412 (1.26 ×) |
| lowThrust_5 | 16,262 | 16,262 | 198,369 | 2 | 100.0 | 25,284 (12.7%) | 83 (1.03×) | <u>77</u> (1.03×) | 82 (1.01×) | 124 (1.20 ×) | 304,740 (1.00×) | 31,485 (0.95×) | <u>26,461</u> (1.05 ×) |
| lowThrust_6 | 16,928 | 16,928 | 207,349 | 2 | 100.0 | 26,320 (12.7%) | 88 (1.03×) | <u>81</u> (1.03×) | 87 (1.00×) | 126 (1.20 ×) | 336,694 (1.00×) | 33,009 (0.95×) | <u>27,873</u> (1.03 ×) |
| lowThrust_7 | 17,378 | 17,378 | 211,561 | 2 | 100.0 | 27,020 (12.8%) | 90 (1.03×) | <u>83</u> (1.03×) | 88 (1.00×) | 129 (1.22 ×) | 192,196 (0.99×) | 34,288 (0.95×) | <u>29,022</u> (1.04 ×) |
| lowThrust_8 | 17,702 | 17,702 | 216,445 | 2 | 100.0 | 27,524 (12.7%) | 92 (1.03×) | <u>85</u> (1.03×) | 91 (0.99×) | 135 (1.20 ×) | 52,778 (0.97×) | 34,946 (0.95×) | <u>29,693</u> (1.04 ×) |
| lowThrust_9 | 18,044 | 18,044 | 219,589 | 2 | 100.0 | 28,056 (12.8%) | 93 (1.03×) | <u>86</u> (1.03×) | 93 (0.97×) | 135 (1.21 ×) | 379,661 (1.00×) | 36,467 (0.93×) | <u>30,575</u> (1.04 ×) |
| lowThrust_10 | 18,260 | 18,260 | 222,005 | 2 | 100.0 | 28,392 (12.8%) | 95 (1.03×) | <u>87</u> (1.03×) | 91 (1.02×) | 136 (1.21 ×) | 81,344 (1.04 ×) | 36,571 (0.95×) | <u>30,897</u> (1.04×) |
| lowThrust_11 | 18,368 | 18,368 | 223,801 | 2 | 100.0 | 28,560 (12.8%) | 96 (1.02×) | <u>88</u> (1.03×) | 94 (0.99×) | 140 (1.20 ×) | 60,631 (1.03 ×) | 36,797 (0.95×) | <u>31,466</u> (1.03×) |
| lowThrust_12 | 18,458 | 18,458 | 219,589 | 2 | 100.0 | 28,700 (12.8%) | 96 (1.03×) | <u>88</u> (1.03×) | 94 (1.01×) | 139 (1.20 ×) | 199,906 (1.00×) | 37,009 (0.95×) | <u>30,715</u> (1.03 ×) |
| lowThrust_13 | 18,476 | 18,476 | 224,897 | 2 | 100.0 | 28,728 (12.8%) | 96 (1.02×) | <u>89</u> (1.03×) | 95 (0.99×) | 139 (1.20 ×) | 398,446 (1.00×) | 37,296 (0.95×) | <u>30,657</u> (1.06 ×) |
| lp_osa_14 | 2,337 | 54,797 | 317,097 | 1 | 73.1 | 38,331 (12.1%) | <u>224</u> (1.09 ×) | 115 (1.01×) | <u>112</u> (1.01×) | 486 (0.96×) | 210,634 (0.95×) | <u>92,705</u> (0.98×) | 243,491 (1.11 ×) |
| lp_osa_30 | 4,350 | 104,374 | 604,488 | 1 | 72.5 | 72,552 (12.0%) | 485 (1.09 ×) | 239 (1.01×) | <u>236</u> (1.00×) | 966 (0.98×) | 654,797 (1.01×) | <u>186,154</u> (0.98×) | 503,332 (1.11 ×) |
| heart2 | 2,339 | 2,339 | 682,797 | 12 | 79.0 | 227,043 (33.3%) | 436 (1.31 ×) | 227 (1.05×) | <u>225</u> (1.05×) | 391 (1.20×) | <u>19,396</u> (1.01×) | <u>35,484</u> (1.37×) | 36,406 (1.48 ×) |
| heart3 | 2,339 | 2,339 | 682,797 | 15 | 79.4 | 235,602 (34.5%) | 419 (1.32 ×) | 227 (1.05×) | <u>225</u> (1.05×) | 389 (1.21×) | <u>19,174</u> (1.03×) | 35,315 (1.38×) | 35,676 (1.51 ×) |
| std1_Jac2 | 21,982 | 21,982 | 1,248,731 | 28 | 60.9 | 183,135 (14.7%) | 987 (1.09×) | 509 (0.99×) | <u>497</u> (0.97×) | 867 (1.19 ×) | 598,588 (1.01×) | <u>97,147</u> (1.34 ×) | 160,722 (1.32×) |
| heart1 | 3,557 | 3,557 | 1,387,773 | 12 | 77.4 | 231,360 (16.7%) | 1,059 (1.10 ×) | 517 (1.04×) | <u>504</u> (1.05×) | 855 (1.12×) | <u>41,565</u> (1.01×) | <u>93,307</u> (1.19×) | 120,122 (1.37 ×) |
| std1_Jac3 | 21,982 | 21,982 | 1,455,848 | 27 | 87.9 | 170,533 (11.7%) | 1,213 (1.09×) | 595 (1.03×) | <u>584</u> (1.00×) | 1,019 (1.12 ×) | 601,773 (1.01×) | <u>115,609</u> (1.34 ×) | 221,053 (1.32×) |
| Zd_Jac2 | 22,835 | 22,835 | 1,642,833 | 34 | 83.7 | 204,812 (12.5%) | 1,350 (1.09×) | 687 (1.07×) | <u>673</u> (1.07×) | 1,183 (1.15 ×) | 604,186 (1.03×) | <u>121,688</u> (1.36 ×) | 224,353 (1.31×) |
| Zd_Jac6 | 22,835 | 22,835 | 1,711,983 | 34 | 89.0 | 217,538 (12.7%) | 1,394 (1.10×) | <u>719</u> (1.09×) | 728 (1.16 ×) | 1,221 (1.09×) | 605,426 (1.02×) | <u>129,535</u> (1.36 ×) | 250,010 (1.31×) |
| Zd_Jac3 | 22,835 | 22,835 | 1,916,152 | 34 | 89.0 | 217,532 (11.4%) | 1,575 (1.09 ×) | 859 (1.05×) | <u>830</u> (1.06×) | 1,432 (1.06×) | 623,166 (1.00×) | <u>149,954</u> (1.35 ×) | 294,195 (1.32×) |
| exdata_1 | 6,001 | 6,001 | 2,269,501 | 1 | 100.0 | 2,253,000 (99.3%) | <u>523</u> (3.90 ×) | <u>513</u> (2.04×) | 513 (2.00×) | 586 (1.91×) | 49,095 (1.39×) | <u>26,707</u> (9.72×) | <u>26,642</u> (25.77 ×) |

densities between 56% and 100%. Block coverage—the fraction of non-zeros residing in δ -dense blocks—varies widely, from 11% to 99%.

Kernels. We evaluate SABLE on two widely used sparse matrix operations. Sparse Matrix-Vector multiplication (SpMV) computes $y_i = \sum_j A_{ij} \cdot x_j$, and is commonly used by iterative solvers [40], graph algorithms such as PageRank [32], and scientific computing [21, 27, 33, 54]. Sparse Matrix-Matrix multiplication (SpMM) computes $y_{ik} = \sum_j A_{ij} \cdot x_{jk}$, where A is sparse and X is dense, and is a fundamental building block of machine learning [18, 53], graph processing [43], and iterative solvers [1, 2]. To demonstrate the practical applicability of our approach, we focus on evaluating the SpMV and SpMM operations, due to the commutative and associative nature of the $+$ operator, which allows us to demonstrate the capabilities of our system without having to solve an orthogonal data dependency problem.

Baselines. We compare SABLE against the following baselines.

- **UZP** [36] (*SpMV*): An inspector-executor system that represents structured regions of a sparse matrix as sets of polyhedra while keeping irregular elements in CSR or COO. In contrast, SABLE identifies δ -dense rectangular blocks.

- **Intel MKL** [51] (*SpMV + SpMM*): The vendor-optimized sparse BLAS implementation in Intel oneAPI Math Kernel Library.
- **SpV8** [25] (*SpMV*): A CSR-based SpMV implementation that uses AVX-512 gather instructions for vectorized column access. Removing non-zero elements from a matrix stored in CSR does not always translate to a proportional SpMV speedup due to effects such as branch mispredictions; SpV8’s branchless vectorized design achieves close to expected linear relationship. This makes SpV8 a particularly informative comparison point for our approach, which relies on the sparse dispatch becoming proportionally faster as non-zeros are moved into δ -dense blocks.
- **Sparse Register Tiling (SpReg)** [55] (*SpMM*): A code generator that mines for submatrices with similar sparsity patterns and constructs regular loops over them using an unroll-and-parse-jam technique.
- **Naive** (*SpMV + SpMM*): A textbook CSR-based implementation.

We did not include techniques [3, 9, 45] that were previously shown to perform worse than one of our baselines.

Implementation. SABLE’s partitioner requires the δ -dense blocks of a matrix to account for at least 10% of its total non-zeros, as below this threshold, the overhead of dense execution tends to

outweigh its performance benefits. subsection 6.3 explores this design decision in more detail. SABLE dispatches δ -dense blocks to either optimized BLAS routines (e.g., `cb1as_dgemv` for SpMV, `cb1as_dgemm` for SpMM) or shape-specialized handwritten kernels, based on the dimensions of the block; the sparse region is dispatched to one of the baselines described above. The SABLE runtime (Section 2) takes as input the operation to perform (SpMV or SpMM) and a sparse library—one of the baselines listed above in our evaluation—enabling users to pair SABLE’s dense block optimizations with any sparse library of their choice.

6.1 Single-Threaded Performance (RQ1)

To compare our approach to existing techniques for structured sparse matrix computation, we applied SABLE to the 70 matrices in our benchmark suite. SABLE’s partitioner identified 30 matrices as potentially benefiting from our approach; Table 1 gives the relative speedup of SABLE over each of our baselines. In general, SABLE improves over every baseline on the majority of benchmarks for both SpMV and SpMM. The largest gains come from matrices with high block coverage: *exdata_1* (99.3% of non-zeros in δ -dense blocks) achieves 3.90 \times for SpMV and 25.77 \times for SpMM, while *jendrec1* (88.1%) achieves 1.79 \times and 2.14 \times , respectively. Even matrices with modest block coverage (11–13%, e.g., the *lowThrust* and *Zd_Jac* families) show consistent improvements of 1.02–1.36 \times . Figure 7 further contextualizes these results, reporting the single-threaded speedup of the best SABLE configuration over the best fully-sparse baseline for each matrix. Here, the best SABLE configuration is the fastest combination of SABLE’s dense dispatch for δ -dense blocks and a sparse library for the remaining region, while the best fully-sparse baseline is the fastest baseline applied to the entire matrix. Each bar is annotated with “SABLE’s sparse dispatch vs best baseline”, indicating which sparse library SABLE used and which fully-sparse baseline was fastest.

For SpMV, SABLE achieves a geometric mean speedup of 1.07 \times over the best fully-sparse baseline, with speedups on 29 out of 30 matrices. The largest SpMV gain is on *exdata_1* (2.01 \times), where 99.3% of non-zeros reside in a single dense block, allowing SABLE to dispatch nearly all computation to `cb1as_dgemv`. Matrices with high block coverage (e.g., *jendrec1* at 88.1%, *eris1176* at 56.2%) also show substantial gains. For matrices with lower block coverage (the percentage of non-zeros residing in δ -dense blocks) (e.g., the *lowThrust* family at \sim 13%), SABLE still achieves consistent speedups of 1.02–1.05 \times over the best SpMV baseline by accelerating just the dense portion. The *lp_osa* matrices show minimal SpMV improvement (1.01 \times) because their blocks cover only \sim 12% of non-zeros and the matrices are highly rectangular, limiting the benefit of dense dispatch. *std1_Jac2* is the sole SpMV slowdown (0.97 \times): its blocks average only 61% density, so the dense kernel spends significant computation on zeros, and the savings from shrinking the sparse problem do not compensate. The *lp_osa* matrices have similarly low block density (73%) but their single-row blocks make the SpMV dense cost negligible, yielding marginal gains (1.01 \times).

For SpMM, SABLE achieves a geometric mean speedup of 1.19 \times , with gains on 27 out of 30 matrices. SpMM generally shows larger speedups than SpMV, as the dense kernel benefits from greater data reuse across the columns of the output matrix. The *heart* matrices

show modest SpMM gains over SpReg because their high ratio of non-zeros to matrix columns allows SpReg’s packing overhead to be amortized effectively. The *lp_osa_07* and *lp_osa_14* matrices are the only SpMM slowdowns (0.92 \times and 0.95 \times), due to their low block coverage (\approx 12%) and low block density (\approx 73%). The largest SpMM gain is on *exdata_1* (2.56 \times over SpReg), followed by *jendrec1* (2.09 \times) and *c-30* (2.02 \times). The *Zd_Jac* and *std1_Jac* families show consistent SpMM speedups of 1.31–1.36 \times despite modest block coverage (11–15%), as SpMM benefits more from the cache locality of dense block storage.

These results confirm that SABLE improves performance over prior approaches on real-world matrices for both SpMV and SpMM, with the magnitude of improvement correlating primarily with the fraction of non-zeros captured in δ -dense blocks (RQ1).

6.2 Parallelization (RQ2)

To understand how SABLE scales when parallelized, we measure the speedup of SABLE over the best fully-sparse baseline at multiple thread counts for both SpMV and SpMM.²

SABLE parallelizes in different ways: δ -dense blocks use either BLAS’s built-in multithreading if dispatched to a BLAS kernel, or OpenMP to parallelize the iteration over the outer dimension of a handwritten kernel; the sparse dispatch uses its own parallelization (e.g., MKL sparse, UZP). Figure 8 shows the per-matrix speedup of SABLE over the best fully-sparse baseline at 8 threads for both SpMV and SpMM, we choose 8 because this is the thread count at which the baselines we evaluated on achieve their best average scaling across our benchmark matrices.

For SpMV, SABLE achieves speedups on 20 of 30 matrices at 8 threads, with the largest gains on *jendrec1* (6.4 \times) and *exdata_1* (3.0 \times). For SpMM, SABLE achieves speedups on 15 of 30 matrices, with the largest gains on *exdata_1* (6.8 \times) and *c-30* (2.4 \times). Matrices that slow down are those with low block coverage, where the sparse portion dominates and scales well on its own.

Figure 9 shows the thread scaling behavior of all SABLE sparse dispatches and fully-sparse baselines for four representative matrices, with SpMV in the top row and SpMM in the bottom row. For *orani678* (90K nnz), parallelism overhead dominates SpMV due to the small matrix size, and all configurations degrade beyond 2 threads; however, SpMM’s higher arithmetic intensity allows SABLE to maintain an advantage, reaching 5.6 \times at 12 threads versus 3.8 \times for fully-sparse. *exdata_1* (2.3M nnz, 99.3% in blocks) shows the most dramatic scaling: since nearly all computation is dispatched to dense BLAS, SABLE achieves \sim 20 \times SpMV and \sim 68 \times SpMM speedup at 12 threads, while fully-sparse baselines plateau at 5 \times and 11 \times , respectively. For *brainpc2* (179K nnz, 30.8% in blocks), SABLE with UZP sparse dispatch scales to nearly 2 \times for SpMV at 12 threads, outpacing all fully-sparse baselines; for SpMM, however, fully-sparse overtakes SABLE at higher thread counts (3.0 \times vs 2.8 \times at 12 threads), as the large number of rows (27,607) gives the fully-sparse baseline ample row-level parallelism, while only 30.8% of non-zeros benefit from dense dispatch. For *Zd_Jac2* (1.6M nnz, only 12.5% in blocks), the fully-sparse Naive baseline scales competitively for SpMV (3.8 \times vs 2.5–3 \times for SABLE at 12 threads),

²We exclude SpReg from this comparison, as we were unable to integrate its parallelization with our system.

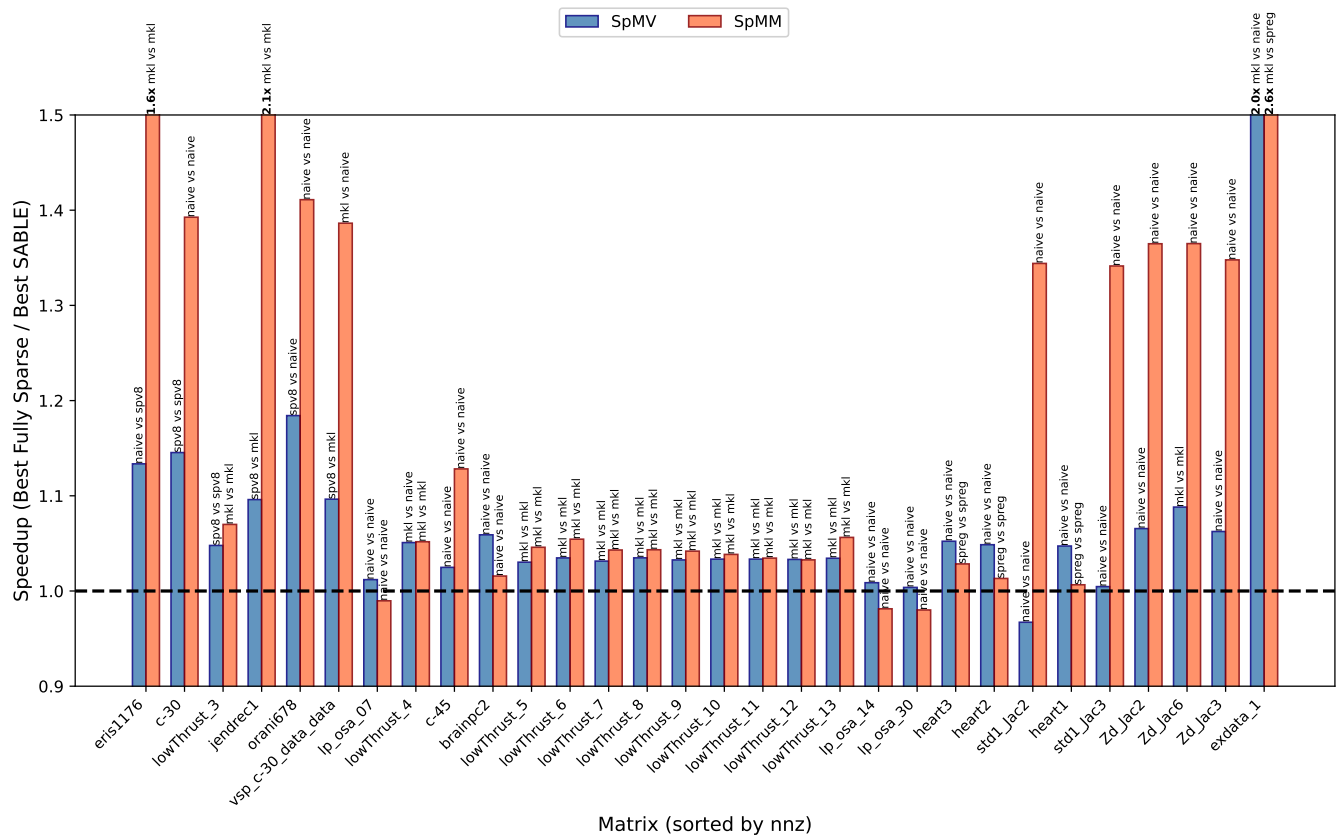


Figure 7: Single-threaded speedup of SABLE over the best fully-sparse baseline for SpMV (geometric mean 1.07 \times) and SpMM (geometric mean 1.19 \times). Each bar is annotated with “SABLE’s sparse dispatch vs best baseline”. Benchmarks whose speedup exceeds the y-axis’s 1.5 \times threshold are labeled with their actual value.

while for SpMM both scale near-linearly with SABLE maintaining a slight edge (11.7 \times vs 11.1 \times).

These results confirm that SABLE’s parallel advantage is strongest when the identified δ -dense blocks constitute a significant fraction of total non-zeros (RQ2).

6.3 Block Coverage Threshold (RQ3)

To validate the design of our partitioner, we consider several variants that change the minimum block-coverage threshold—the fraction of a matrix’s non-zeros that must reside in identified δ -dense blocks for SABLE to accept the matrix for VBR-C conversion (Section 3). We ran SABLE on the full set of 70 randomly selected SuiteSparse matrices—including the 30 matrices in Table 1 and 40 additional matrices whose block coverage fell below 10%—and varied the acceptance threshold from 0% to 20%. Table 2 reports, for each threshold, the number of included matrices, how many SABLE outperforms or underperforms the best fully-sparse baseline, and the geometric-mean speedup.

With no threshold (0%), all 70 matrices are included, but roughly a third exhibit slowdowns (25 for SpMV, 26 for SpMM), dragging the geometric-mean speedups down to 1.03 \times and 1.07 \times . As the threshold increases, the number of slowdowns drops sharply while the

geometric mean rises: at 5% coverage, slowdowns fall to 5 (SpMV) and 14 (SpMM); at 9%, only 2 SpMV and 5 SpMM slowdowns remain. The 10% threshold is the point at which nearly all remaining matrices benefit: 29 of 30 for SpMV (1.07 \times geometric mean) and 26 of 30 for SpMM (1.18 \times). Beyond 12%, the threshold begins to exclude matrices that genuinely benefit from SABLE—at 13%, the included set drops sharply from 28 to 14, eliminating the entire *lowThrust* family (block coverage \sim 12.7%) and several *Zd_jac* matrices that consistently show meaningful speedups (Table 1). The 10% threshold thus provides a principled cutoff: it filters out matrices whose δ -dense blocks cover too few non-zeros to offset the overhead of dense execution, while retaining nearly all matrices where the approach yields consistent improvements.

6.4 Discussion

Table 2 provides evidence that block coverage—the fraction of nonzeros residing in δ -dense blocks—is the primary determinant of whether SABLE improves performance: below 10%, the dense blocks capture too few nonzeros to offset the overhead of format conversion and dense execution, while above 10% almost all matrices benefit. This relationship holds because SABLE achieves speedup when the time saved by shrinking the sparse problem exceeds the

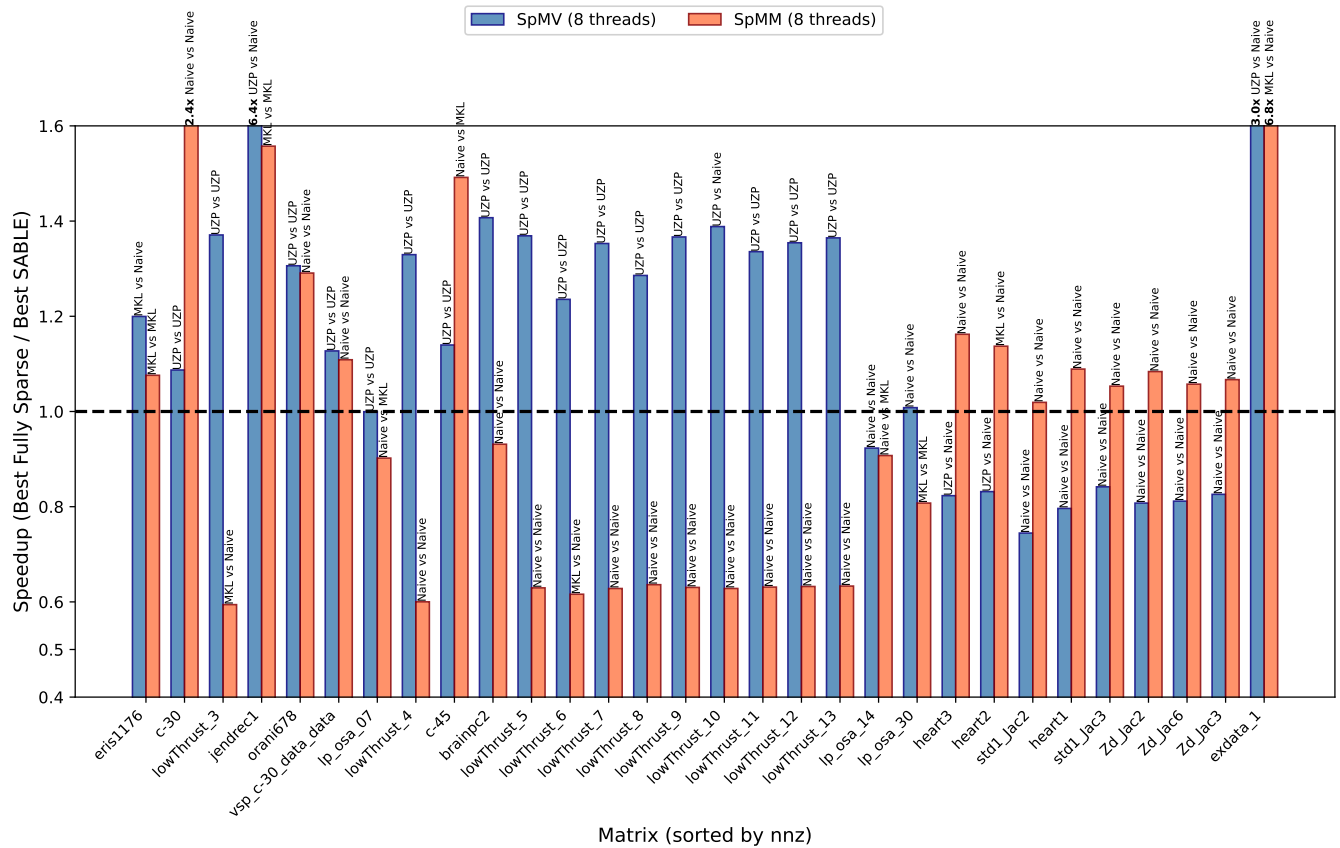


Figure 8: Speedup of SABLE over the best fully-sparse baseline at 8 threads for SpMV and SpMM. Each bar is annotated with “SABLE’s sparse dispatch vs best baseline”. Benchmarks whose speedup exceeds the y-axis’s 1.6× threshold are labeled with their actual value.

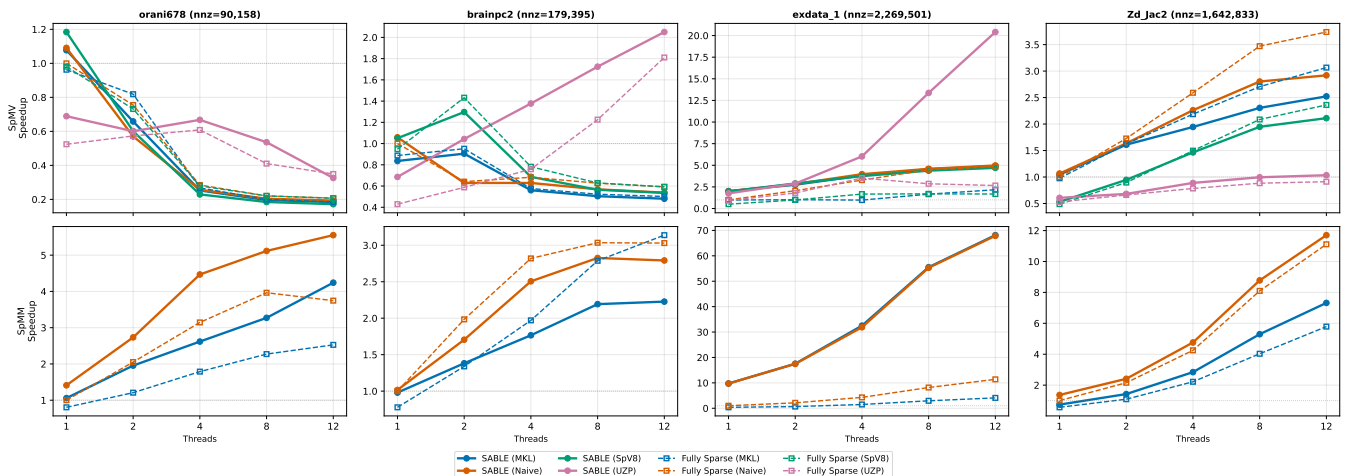


Figure 9: Thread scaling for four representative matrices: SpMV (top row) and SpMM (bottom row). Solid lines show SABLE with different sparse dispatches; dashed lines show the corresponding fully-sparse baselines. All values are speedups over the single-threaded time of the best fully-sparse baseline (higher is better).

Table 2: Effect of the minimum block-coverage threshold on SABLE performance. For each threshold (minimum percentage of non-zeros residing in δ -dense blocks), we report the number of included matrices, how many SABLE outperforms ($>1\times$) or underperforms ($\leq 1\times$) the best fully-sparse baseline, and the geometric-mean speedup.

| Thr. | #Mat. | SpMV | | | SpMM | | |
|------|-------|------------|----------------|---------------|------------|----------------|---------------|
| | | $>1\times$ | $\leq 1\times$ | Geo. mean | $>1\times$ | $\leq 1\times$ | Geo. mean |
| 0% | 70 | 45 | 25 | 1.03 \times | 44 | 26 | 1.07 \times |
| 5% | 41 | 36 | 5 | 1.06 \times | 27 | 14 | 1.11 \times |
| 6% | 40 | 35 | 5 | 1.06 \times | 27 | 13 | 1.11 \times |
| 7% | 39 | 34 | 5 | 1.06 \times | 27 | 12 | 1.11 \times |
| 8% | 35 | 30 | 5 | 1.06 \times | 26 | 9 | 1.13 \times |
| 9% | 31 | 29 | 2 | 1.07 \times | 26 | 5 | 1.18 \times |
| 10% | 30 | 29 | 1 | 1.07 \times | 26 | 4 | 1.18 \times |
| 11% | 30 | 29 | 1 | 1.07 \times | 26 | 4 | 1.18 \times |
| 12% | 28 | 27 | 1 | 1.08 \times | 24 | 4 | 1.17 \times |
| 13% | 14 | 13 | 1 | 1.12 \times | 13 | 1 | 1.28 \times |
| 14% | 12 | 11 | 1 | 1.13 \times | 11 | 1 | 1.32 \times |
| 15% | 11 | 11 | 0 | 1.14 \times | 10 | 1 | 1.31 \times |
| 20% | 10 | 10 | 0 | 1.16 \times | 10 | 0 | 1.40 \times |

cost of running the dense kernel on the extracted blocks. Higher coverage means more nonzeros move from sparse indexing to dense computation, increasing the savings. At the extreme, `exdata_1`—a $6,001 \times 6,001$ matrix where a single $1,501 \times 1,501$ block captures 99.3% of all nonzeros—achieves $25.77\times$ SpMM and $3.90\times$ SpMV speedup (Table 1).

While coverage determines how much work moves to the dense kernel, block dimensions determine the cost of performing that work. This effect is pronounced for SpMM but largely absent for SpMV. The `Zd_Jac` and `lowThrust` benchmarks illustrate this phenomenon: while they both have ~ 12 – 13% block coverage, shapes of those blocks differ dramatically. The `Zd_Jac` matrices contain 34 blocks of 30×240 , and the SpMM dense kernel processes them at approximately 27 ns/nnz, yielding a $1.31\times$ average speedup. The `lowThrust` matrices contain just 2 blocks of $N \times 2$ and $2 \times N$, where the dense kernel cost rises to ~ 160 ns/nnz— $6\times$ more expensive—yielding a speedup of only $1.04\times$. For SpMV, by contrast, the dense kernel cost is nearly constant across all block shapes (0.23 – 0.32 ns/nnz), so SpMV speedup depends almost entirely on coverage rather than block geometry. Even the most expensive SpMM blocks still produce positive speedup: for the `lowThrust` family, removing $\sim 13\%$ of nonzeros from the sparse path reduces its execution time by $\sim 18\%$ —more than the proportional amount—and these amplified savings cover the cost of the dense kernel.

7 Related Work

Sparse matrix representations. Work in the past has looked into defining new storage formats that facilitate operations over blocked formats—CSB [1], BCSR [22], and SELL-P [2] are fixed-size block formats. Vuduc and Moon [50] developed UBCSR as an extension of the BCSR format studied by Im et al. [20], to reduce the extra zeros (fill-in) that occur with fixed-size blocking and thereby reduce indexing overhead and enable register-level tiling. Our approach

builds on these techniques. TACO [24] and UniSparse [26] provide abstractions over storage formats but cannot represent variable-sized blocks. SparseTIR [57] provides a TACO-like language to specify operations over matrices as a composition of different storage formats based on loop index constructs.

Hybrid storage formats. Several systems compose multiple storage formats to handle heterogeneous structure within a single matrix. LAV [58] stores the dense region of a matrix in a new format, and the sparse region as CSR. TileSpMV [30] and BDMP-PBP [60] divide a matrix into fixed-size blocks and determine the best storage format for each block to improve SpMV performance. STile [15] finds sub-matrices (not necessarily blocks) and an appropriate storage format for them, storing the result as a composition of formats in SparseTIR’s IR. UZP [36] represents the dense regions of the matrix as several equations and the rest as COO or CSR.

Re-ordering matrices for better performance. Other work exists in re-ordering matrices for better performance [16, 59]. SpV8 [25] groups rows of similar density together and dispatches them to kernels with different vectorization strategies, avoiding branch mispredictions from frequently triggering conditionals. VNEC [52] builds on SpV8 and introduces a storage format that chunks rows and reduces empty columns to coalesce elements together. SABLE does not do any re-ordering of the matrix since it simply identifies matrices that have some inherent structure in the form of δ -dense blocks. In the future, re-ordering techniques could be used to create δ -dense block structures in matrices that do not naturally exhibit them.

Inspector-executor. The Inspector-Executor model [35] of performing operations over sparse matrices [48] is well studied, with a lot of work being done in the context of SpMV operations. These approaches aim to generate code that is specialized to the sparsity pattern of the matrix and can be reused for different matrices having the same sparsity pattern. Apart from LCM I/E [9], the most closely related papers are Sparse Register Tiling [55] which uses an unroll-and-sparse-jam technique to generate optimized code that achieves good register reuse without excessive fill-in, and Augustine et al. [3] which tries to build regular polyhedra from a trace of the memory access patterns, that allows the construction of multiple *for-loops* that can reproduce the entire trace. However, the inspection time is too high for larger matrices, and it is only able to construct loops over indices that are regularly stridden. MACVETH [17] extends this line of work by performing a peep-hole optimization over *gather* instructions to facilitate vectorization. There are other widely used bodies of inspector executor systems for operating over sparse tensors such as the Sparse Polyhedral Framework [44–46], Sympiler [10] and ParSy [11].

Staging. Staged metaprogramming is a well studied technique studied in the context of multiple languages - Scala [37], C++ [6], OCaml [23], etc. There have even been previous staging techniques for sparse tensors [31, 38] which this paper draws on however, none of these approaches use metaprogramming to generate code for arbitrary user-defined operations in conjunction with a block iterator as in this paper. Dehame et al. [13] talks about partially evaluating parts of the code involving the sparse tensor operation,

but is limited to some hardcoded rules and does not generalize to arbitrary sparse tensor operations.

8 Conclusion

This work proposes a novel approach towards performing operations over sparse matrices that have some known block structure at compile time. SABLE uses a novel partitioning algorithm to partition sparse matrices into variable-sized blocks stored in the Variable Block Row-Compressed (VBR-C) format, then generates specialized dispatch code based on block features (rows, columns, and δ). For high δ -dense blocks, SABLE dispatches to optimized dense kernels, demonstrating that for certain matrix structures, it is often beneficial to operate over some zeros rather than try and specialize code to avoid computing over any zeros. For low δ -dense blocks, SABLE dispatches to user-supplied sparse kernels, allowing users to leverage any current or future state-of-the-art sparse library. In our evaluations, we demonstrate that we are able to get a significant speedup for SpMV and SpMM operations over our baseline.

References

- [1] Hasan Metin Aktulga, Aydin Buluç, Samuel Williams, and Chao Yang. 2014. Optimizing Sparse Matrix-Multiple Vectors Multiplication for Nuclear Configuration Interaction Calculations. In *2014 IEEE 28th International Parallel and Distributed Processing Symposium*. 1213–1222. <https://doi.org/10.1109/IPDPS.2014.125>
- [2] Hartwig Anzt, Stanimire Tomov, and Jack J. Dongarra. 2014. Implementing a Sparse Matrix Vector Product for the SELL-C / SELL-C- σ formats on NVIDIA GPUs. <https://api.semanticscholar.org/CorpusID:14781903>
- [3] Travis Augustine, Janarthanan Sarma, Louis-Noël Pouchet, and Gabriel Rodriguez. 2019. Generating piecewise-regular code from irregular structures. In *Proceedings of the 40th ACM SIGPLAN Conference on Programming Language Design and Implementation, PLDI 2019, Phoenix, AZ, USA, June 22–26, 2019*, Kathryn S. McKinley and Kathleen Fisher (Eds.). ACM, 625–639. <https://doi.org/10.1145/3314221.3314615>
- [4] Brett W. Bader and Tamara G. Kolda. 2007. Efficient MATLAB Computations with Sparse and Factored Tensors. *SIAM Journal on Scientific Computing* 30, 1 (December 2007), 205–231. <https://doi.org/10.1137/060676489>
- [5] A. H. Baker, J. M. Dennis, and E. R. Jessup. 2006. ON IMPROVING LINEAR SOLVER PERFORMANCE: A BLOCK VARIANT OF GMRES. *Siam Journal On Scientific Computing*, 1608–1626.
- [6] Ajay Brahmakshatriya and Saman Amarasinghe. 2021. BuildIt: A Type-Based Multi-stage Programming Framework for Code Generation in C++. In *2021 IEEE/ACM International Symposium on Code Generation and Optimization (CGO)*, 39–51. <https://doi.org/10.1109/CGO51591.2021.9370333>
- [7] Aydin Buluç, Jeremy T. Fineman, Matteo Frigo, John R. Gilbert, and Charles E. Leiserson. 2009. Parallel sparse matrix-vector and matrix-transpose-vector multiplication using compressed sparse blocks. In *SPAA 2009: Proceedings of the 21st Annual ACM Symposium on Parallelism in Algorithms and Architectures, Calgary, Alberta, Canada, August 11–13, 2009*, Friedhelm Meyer auf der Heide and Michael A. Bender (Eds.). ACM, 233–244. <https://doi.org/10.1145/1583991.1584053>
- [8] Roberto L. Castro, Andrei Ivanov, Diego Andrade, Tal Ben-Nun, Basilio B. Fraguela, and Torsten Hoefer. 2023. VENOM: A Vectorized N:M Format for Unleashing the Power of Sparse Tensor Cores. In *Proceedings of the International Conference for High Performance Computing, Networking, Storage and Analysis (Denver, CO, USA) (SC '23)*. Association for Computing Machinery, New York, NY, USA, Article 72, 14 pages. <https://doi.org/10.1145/3581784.3607087>
- [9] Kazem Cheshmi, Zachary Cetinic, and Maryam Mehri Dehnavi. 2022. Vectorizing Sparse Matrix Computations with Partially-Strided Codelets. In *SC22: International Conference for High Performance Computing, Networking, Storage and Analysis*. 1–15. <https://doi.org/10.1109/SC41404.2022.00037>
- [10] Kazem Cheshmi, Shoaib Kamil, Michelle Mills Strout, and Maryam Mehri Dehnavi. 2017. Sympiler: transforming sparse matrix codes by decoupling symbolic analysis. In *Proceedings of the International Conference for High Performance Computing, Networking, Storage and Analysis (Denver, Colorado) (SC '17)*. Association for Computing Machinery, New York, NY, USA, Article 13, 13 pages. <https://doi.org/10.1145/3126908.3126936>
- [11] Kazem Cheshmi, Shoaib Kamil, Michelle Mills Strout, and Maryam Mehri Dehnavi. 2018. ParSy: inspection and transformation of sparse matrix computations for parallelism. In *Proceedings of the International Conference for High Performance Computing, Networking, Storage, and Analysis, SC 2018, Dallas, TX, USA, November 11–16, 2018*. IEEE / ACM, 62:1–62:15. <http://dl.acm.org/citation.cfm?id=3291739>
- [12] Timothy A. Davis and Yifan Hu. 2011. The university of Florida sparse matrix collection. *ACM Trans. Math. Softw.* 38, 1, Article 1 (Dec. 2011), 25 pages. <https://doi.org/10.1145/2049662.2049663>
- [13] Gabriel Dehame, Christophe Alias, and Alec Sadler. 2023. *Partial Evaluation of Dense Code on Sparse Structures*. Technical Report RR-9534. INRIA Lyon ; CNRS ; ENS de Lyon ; Université de Lyon. 16 pages. <https://inria.hal.science/hal-04358187>
- [14] S. C. Eisenstat, M. C. Gursky, M. H. Schultz, and A. H. Sherman. 1982. Yale sparse matrix package I: The symmetric codes. *Internat. J. Numer. Methods Engrg.* 18, 8 (1982), 1145–1151. <https://doi.org/10.1002/nme.1620180804> arXiv:<https://onlinelibrary.wiley.com/doi/pdf/10.1002/nme.1620180804>
- [15] Jingzhi Fang, Yanyan Shen, Yue Wang, and Lei Chen. 2024. STile: Searching Hybrid Sparse Formats for Sparse Deep Learning Operators Automatically. *Proc. ACM Manag. Data* 2, 1 (2024), 68:1–68:26. <https://doi.org/10.1145/3639323>
- [16] Changwan Hong, Aravind Sukumaran-Rajam, Israt Nisa, Kunal Singh, and P. Sadayappan. 2019. Adaptive sparse tiling for sparse matrix multiplication. In *Proceedings of the 24th Symposium on Principles and Practice of Parallel Programming (Washington, District of Columbia) (PPoPP '19)*. Association for Computing Machinery, New York, NY, USA, 300–314. <https://doi.org/10.1145/3293883.3295712>
- [17] Marcos Horro, Louis-Noël Pouchet, Gabriel Rodriguez, and Juan Touriño. 2022. Custom High-Performance Vector Code Generation for Data-Specific Sparse Computations. In *Proceedings of the International Conference on Parallel Architectures and Compilation Techniques, PACT 2022, Chicago, Illinois, October 8–12, 2022*, Andreas Klöckner and José Moreira (Eds.). ACM, 160–171. <https://doi.org/10.1145/3559009.3569668>
- [18] Yuwei Hu, Zihao Ye, Minjie Wang, Jiali Yu, Da Zheng, Mu Li, Zheng Zhang, Zhiru Zhang, and Yida Wang. 2020. FeatGraph: A Flexible and Efficient Backend for Graph Neural Network Systems. In *SC20: International Conference for High Performance Computing, Networking, Storage and Analysis*. 1–13. <https://doi.org/10.1109/SC41405.2020.00075>
- [19] Kezhao Huang, Jidong Zhai, Zhen Zheng, Youngmin Yi, and Xipeng Shen. 2021. Understanding and bridging the gaps in current GNN performance optimizations. In *Proceedings of the 26th ACM SIGPLAN Symposium on Principles and Practice of Parallel Programming (Virtual Event, Republic of Korea) (PPoPP '21)*. Association for Computing Machinery, New York, NY, USA, 119–132. <https://doi.org/10.1145/3437801.3441585>
- [20] Eun-Jin Im, Katherine A. Yelick, and Richard W. Vuduc. 2004. Sparsity: Optimization Framework for Sparse Matrix Kernels. *Int. J. High Perform. Comput. Appl.* 18, 1 (2004), 135–158. <https://doi.org/10.1177/1094342004041296>
- [21] Eun-Jin Im. 2000. *Optimizing the Performance of Sparse Matrix-Vector Multiplication*. Ph. D. Dissertation. EECS Department, University of California, Berkeley. <http://www2.eecs.berkeley.edu/Pubs/TechRpts/2000/5556.html>
- [22] Eun-Jin Im and Katherine A. Yelick. 2000. *Optimizing the Performance of Sparse Matrix-Vector Multiplication*. Ph. D. Dissertation. AAI9979665.
- [23] Oleg Kiselyov. 2023. MetaOCaml Theory and Implementation. arXiv:2309.08207 [cs.PL]
- [24] Fredrik Kjolstad, Shoaib Kamil, Stephen Chou, David Lugato, and Saman Amarasinghe. 2017. The tensor algebra compiler. *Proc. ACM Program. Lang.* 1, OOPSLA, Article 77 (oct 2017), 29 pages. <https://doi.org/10.1145/3133901>
- [25] Chenyang Li, Tian Xia, Wenzhe Zhao, Nanning Zheng, and Pengyu Ren. 2021. SpV8: Pursuing Optimal Vectorization and Regular Computation Pattern in SpMV. In *2021 58th ACM/IEEE Design Automation Conference (DAC)*. 661–666. <https://doi.org/10.1109/DAC18074.2021.9586251>
- [26] Jie Liu, Zhongyuan Zhao, Zijian Ding, Benjamin Brock, Hongbo Rong, and Zhiru Zhang. 2024. UniSparse: An Intermediate Language for General Sparse Format Customization. *Proc. ACM Program. Lang.* 8, OOPSLA1 (2024), 137–165. <https://doi.org/10.1145/3649816>
- [27] Weifeng Liu and Brian Vinter. 2015. CSR5: An Efficient Storage Format for Cross-Platform Sparse Matrix-Vector Multiplication. In *Proceedings of the 29th ACM on International Conference on Supercomputing (Newport Beach, California, USA) (ICS '15)*. Association for Computing Machinery, New York, NY, USA, 339–350. <https://doi.org/10.1145/2751205.2751209>
- [28] Simon Moll, Shrey Sharma, Matthias Kurtenacker, and Sebastian Hack. 2019. Multi-dimensional Vectorization in LLVM. In *Proceedings of the 5th Workshop on Programming Models for SIMD/Vector Processing (Washington, DC, USA) (WP-MVP'19)*. Association for Computing Machinery, New York, NY, USA, Article 3, 8 pages. <https://doi.org/10.1145/3303117.3306172>
- [29] Rajesh Nishtala, Richard W. Vuduc, James Demmel, and Katherine A. Yelick. 2007. When cache blocking of sparse matrix vector multiply works and why. *Appl. Algebra Eng. Commun. Comput.* 18, 3 (2007), 297–311. <https://doi.org/10.1007/S00200-007-0038-9>
- [30] Yuyao Niu, Zhengyang Lu, Meichen Dong, Zhou Jin, Weifeng Liu, and Guangming Tan. 2021. TileSpMV: A Tiled Algorithm for Sparse Matrix-Vector Multiplication on GPUs. In *35th IEEE International Parallel and Distributed Processing Symposium, IPDPS 2021, Portland, OR, USA, May 17–21, 2021*. IEEE, 68–78. <https://doi.org/10.1109/IPDPS49936.2021.00016>
- [31] Leo Osvald and Tiark Rompf. 2017. Flexible data views: design and implementation. In *Proceedings of the 4th ACM SIGPLAN International Workshop*

- on Libraries, Languages, and Compilers for Array Programming, ARRAY@PLDI 2017, Barcelona, Spain, June 18, 2017, Martin Elsman, Clemens Grellck, Andreas Klöckner, David A. Padua, and Edgar Solomonik (Eds.). ACM, 25–32. <https://doi.org/10.1145/3091966.3091970>
- [32] Larry Page, Sergey Brin, Rajeev Motwani, and Terry Winograd. 1999. The PageRank Citation Ranking: Bringing Order to the Web. In *Technical Report*. <http://ilpubs.stanford.edu:8090/422/>
- [33] Ali Pinar and Michael T. Heath. 1999. Improving Performance of Sparse Matrix-Vector Multiplication. In *Proceedings of the 1999 ACM/IEEE Conference on Supercomputing* (Portland, Oregon, USA) (SC '99). Association for Computing Machinery, New York, NY, USA, 30–es. <https://doi.org/10.1145/331532.331562>
- [34] Ali Pinar and Virginia Vassilevska. 2004. Finding nonoverlapping substructures of a sparse matrix. *Electronic Transactions on Numerical Analysis* 21 (8 2004). <https://www.osti.gov/biblio/886963>
- [35] R. Ponnusamy, J. Saltz, and A. Choudhary. 1993. Runtime compilation techniques for data partitioning and communication schedule reuse. In *Proceedings of the 1993 ACM/IEEE Conference on Supercomputing* (Portland, Oregon, USA) (Supercomputing '93). Association for Computing Machinery, New York, NY, USA, 361–370. <https://doi.org/10.1145/169627.169752>
- [36] Alonso Rodriguez-Iglesias, Santoshkumar T. Tongli, Emily Tucker, Louis-Noël Pouchet, Gabriel Rodriguez, and Juan Touriño. 2025. Modular Construction and Optimization of the UZP Sparse Format for SpMV on CPUs. *Proc. ACM Program. Lang.* 9, PLDI, Article 232 (June 2025), 25 pages. <https://doi.org/10.1145/3729335>
- [37] Tiark Rompf and Martin Odersky. 2012. Lightweight modular staging: a pragmatic approach to runtime code generation and compiled DSLs. *Commun. ACM* 55, 6 (2012), 121–130. <https://doi.org/10.1145/2184319.2184345>
- [38] Tiark Rompf, Arvind K. Sujeth, Nada Amin, Kevin J. Brown, Vojin Jovanovic, Hyoukjoong Lee, Manohar Jonnalagedda, Kunle Olukotun, and Martin Odersky. 2013. Optimizing data structures in high-level programs: new directions for extensible compilers based on staging. In *Proceedings of the 40th Annual ACM SIGPLAN-SIGACT Symposium on Principles of Programming Languages* (Rome, Italy) (POPL '13). Association for Computing Machinery, New York, NY, USA, 497–510. <https://doi.org/10.1145/2429069.2429128>
- [39] Youcef Saad. 1994. SPARSKIT: A basic tool kit for sparse matrix computations. *Technical Report* (1994).
- [40] Yousef Saad. 2003. *Iterative Methods for Sparse Linear Systems* (2nd ed.). SIAM. <https://doi.org/10.1137/1.9780898718003>
- [41] Ahmet Erdem Sariyüce, Erik Saule, Kamer Kaya, and Ümit V. Çatalyürek. 2015. Regularizing graph centrality computations. *J. Parallel Distributed Comput.* 76 (2015), 106–119. <https://doi.org/10.1016/j.jpdc.2014.07.006>
- [42] M. Shantharam, A. Chatterjee, and P. Raghavan. 2011. Exploiting Dense Substructures for Fast Sparse Matrix Vector Multiplication. *The International Journal of High Performance Computing Applications* 25, 3 (2011), 328–341. <https://doi.org/10.1177/1094342011414748>
- [43] Julian Shun and Guy E. Blelloch. 2013. Ligra: a lightweight graph processing framework for shared memory. 48, 8 (feb 2013), 135–146. <https://doi.org/10.1145/2517327.2442530>
- [44] Michelle Mills Strout, Geri Georg, and Catherine Olschanowsky. 2013. Set and Relation Manipulation for the Sparse Polyhedral Framework. In *Languages and Compilers for Parallel Computing*, Hironori Kasahara and Keiji Kimura (Eds.). Springer Berlin Heidelberg, Berlin, Heidelberg, 61–75.
- [45] Michelle Mills Strout, Mary Hall, and Catherine Olschanowsky. 2018. The Sparse Polyhedral Framework: Composing Compiler-Generated Inspector-Executor Code. *Proc. IEEE* 106, 11 (2018), 1921–1934. <https://doi.org/10.1109/JPROC.2018.2857721>
- [46] Michelle Mills Strout, Alan LaMielle, Larry Carter, Jeanne Ferrante, Barbara Kreaseck, and Catherine Olschanowsky. 2016. An approach for code generation in the Sparse Polyhedral Framework. *Parallel Comput.* 53 (2016), 32–57. <https://doi.org/10.1016/j.parco.2016.02.004>
- [47] Walid Taha and Tim Sheard. 1997. Multi-Stage Programming. In *Proceedings of the 1997 ACM SIGPLAN International Conference on Functional Programming (ICFP '97)*, Amsterdam, The Netherlands, June 9-11, 1997, Simon L. Peyton Jones, Mads Tofte, and A. Michael Berman (Eds.). ACM, 321. <https://doi.org/10.1145/258948.258990>
- [48] M. Ujaldon, S. D. Sharma, J. Saltz, and E. L. Zapata. 1995. Run-time techniques for parallelizing sparse matrix problems. In *Parallel Algorithms for Irregularly Structured Problems*, Afonso Ferreira and José Rolim (Eds.). Springer Berlin Heidelberg, Berlin, Heidelberg, 43–57.
- [49] Richard Wilson Vuduc and James W. Demmel. 2003. *Automatic performance tuning of sparse matrix kernels*. Ph.D. Dissertation. AAI3121741.
- [50] Richard W. Vuduc and Hyun-Jin Moon. 2005. Fast Sparse Matrix-Vector Multiplication by Exploiting Variable Block Structure. In *High Performance Computing and Communications*, Laurence T. Yang, Omer F. Rana, Beniamino Di Martino, and Jack Dongarra (Eds.). Springer Berlin Heidelberg, Berlin, Heidelberg, 807–816.
- [51] Endong Wang, Qing Zhang, Bo Shen, Guangyong Zhang, Xiaowei Lu, Qing Wu, and Yajuan Wang. 2014. *Intel Math Kernel Library*. Springer International Publishing, Cham, 167–188. https://doi.org/10.1007/978-3-319-06486-4_7
- [52] Luhan Wang, Haipeng Jia, Lei Xu, Cunyang Wei, Kun Li, Xianmeng Jiang, and Yunquan Zhang. 2024. VNEC: A Vectorized Non-Empty Column Format for SpMV on CPUs. In *2024 IEEE International Parallel and Distributed Processing Symposium (IPDPS)*, 14–25. <https://doi.org/10.1109/IPDPS57955.2024.00011>
- [53] Minjie Wang, Lingfan Yu, Da Zheng, Quan Gan, Yu Gai, Zihao Ye, Mufei Li, Jinjing Zhou, Qi Huang, Chao Ma, Ziyue Huang, Qipeng Guo, Hao Zhang, Haibin Lin, Junbo Zhao, Jinyang Li, Alexander J. Smola, and Zheng Zhang. 2019. Deep Graph Library: Towards Efficient and Scalable Deep Learning on Graphs. *CoRR* abs/1909.01315 (2019). arXiv:1909.01315 <http://arxiv.org/abs/1909.01315>
- [54] J.B. White and P. Sadayappan. 1997. On improving the performance of sparse matrix-vector multiplication. In *Proceedings Fourth International Conference on High-Performance Computing*, 66–71. <https://doi.org/10.1109/HIPC.1997.634472>
- [55] Lucas Wilkinson, Kazem Cheshmi, and Maryam Mehri Dehnavi. 2023. Register Tiling for Unstructured Sparsity in Neural Network Inference. *Proc. ACM Program. Lang.* 7, PLDI, Article 188 (June 2023), 26 pages. <https://doi.org/10.1145/3591302>
- [56] Michael E. Wolf and Monica S. Lam. 1991. A Data Locality Optimizing Algorithm. In *Proceedings of the ACM SIGPLAN'91 Conference on Programming Language Design and Implementation (PLDI)*, Toronto, Ontario, Canada, June 26-28, 1991, David S. Wise (Ed.). ACM, 30–44. <https://doi.org/10.1145/113445.113449>
- [57] Zihao Ye, Ruihang Lai, Junru Shao, Tianqi Chen, and Luis Ceze. 2023. SparseTIR: Composable Abstractions for Sparse Compilation in Deep Learning. In *Proceedings of the 28th ACM International Conference on Architectural Support for Programming Languages and Operating Systems, Volume 3* (Vancouver, BC, Canada) (ASPLoS 2023). Association for Computing Machinery, New York, NY, USA, 660–678. <https://doi.org/10.1145/3582016.3582047>
- [58] Serif Yesil, Azin Heidarshenas, Adam Morrison, and Josep Torrellas. 2020. Speeding Up SpMV for Power-Law Graph Analytics by Enhancing Locality & Vectorization. In *SC20: International Conference for High Performance Computing, Networking, Storage and Analysis*, 1–15. <https://doi.org/10.1109/SC41405.2020.00090>
- [59] A. N. Yzelman and Rob H. Bisseling. 2009. Cache-Oblivious Sparse Matrix-Vector Multiplication by Using Sparse Matrix Partitioning Methods. *SIAM J. Sci. Comput.* 31, 4 (jul 2009), 3128–3154. <https://doi.org/10.1137/080733243>
- [60] Zhixiang Zhao, Guoyin Zhang, Yanxia Wu, Ruize Hong, Yiqing Yang, and Yan Fu. 2024. Block-wise dynamic mixed-precision for sparse matrix-vector multiplication on GPUs. *J. Supercomput.* 80, 10 (2024), 13681–13713. <https://doi.org/10.1007/S11227-024-05949-6>